The Diffraction Pattern of a Double Helix Under Fraunhofer Conditions

23 March 2025

Abstract

Photo 51, the iconic diffraction image of DNA, provided critical evidence for the double-helical structure of nucleic acids. Under the Fraunhofer (far-field) approximation, the measured diffraction intensity of an sample is proportional to the squared magnitude of the Fourier transform of the sample's electron density. In this write-up, we derive the diffraction pattern for an idealized double helix modeled as two coiled δ function wires and demonstrate that the resulting diffraction pattern exhibits the discrete layer lines observed in the famous photograph.

1 Introduction

The structural determination of DNA is one of the most celebrated achievements in modern science. The famous "Photo 51" (shown in Figure 1), obtained by Franklin and Gosling in 1952, revealed an X-shaped diffraction pattern that was pivotal in identifying the double-helical structure of DNA [1, 2]. In diffraction experiments, the measured intensity is (to a good approximation) the squared magnitude of the Fourier transform of the object's electron density. This relationship is rigorously established under the Fraunhofer diffraction approximation.

The Fraunhofer approximation applies when the distance L between the sample (aperture) and the detector satisfies

$$L \gg \frac{D^2}{\lambda},$$

where D is a characteristic dimension of the sample and λ is the wavelength of the incident radiation. Two key assumptions underlie this approximation [3, 4]:

1. **Planar Wavefronts:** The incident radiation is assumed to be a plane wave, so that any curvature in the wavefronts over the extent of the sample can be neglected.

2. **Linear Phase Variation:** The phase difference across the aperture is approximately linear, allowing the spherical wave emanating from the aperture to be approximated locally by a plane wave.

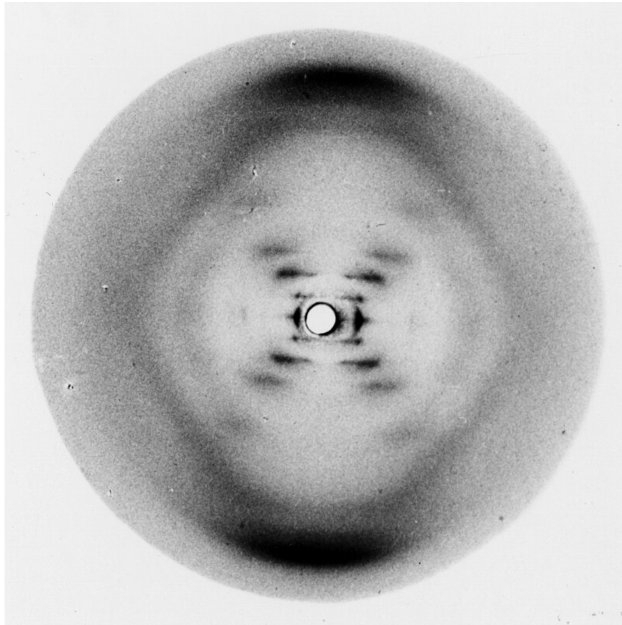

Figure 1: "Photo 51", key evidence in revealing the structure of DNA (Kings College London Archives)

Under these conditions, the complex amplitude $U(P)$ at a point P in the far field is given by the scalar diffraction integral

$$U(P) = \frac{e^{ikL}}{i\lambda L} \int_A U(\mathbf{r}')\, e^{-ik\,\frac{\mathbf{r}\cdot\mathbf{r}'}{L}}\, d^2r',$$

where $\mathbf{r}'$ are coordinates in the aperture plane, $\mathbf{r}$ are coordinates in the detection plane, and $k = 2\pi/\lambda$. Defining the spatial frequency coordinates

$$q_x = \frac{kx}{L}, \quad q_y = \frac{ky}{L},$$

the integral becomes

$$U(P) \propto \int_A U(\mathbf{r}')\, e^{-i(q_x x' + q_y y')}\, d^2r' = \mathcal{F}\{U(\mathbf{r}')\}.$$

Since the measured intensity is

$$I(P) = |U(P)|^2,$$

it follows that

$$I(P) \propto \Big|\mathcal{F}\{U(\mathbf{r}')\}\Big|^2.$$

A full proof of this relationship, including all approximations and assumptions, is given in Osgood's Lectures on Fourier Transform and Its Applications [5]. This fundamental result underpins the interpretation of diffraction experiments: by measuring $I(P)$, one obtains information about the Fourier transform of the sample's electron density and, by inversion, about its structure.

Here, we adopt a coordinate system in which the double helix is aligned along the z-axis and the incident beam is directed along $+z$ (normal incidence). Although real experiments may involve oblique incidence, any such configuration can be rotated into this frame without loss of generality. Our goal is to derive the diffraction pattern for the double helix and show that its Fourier transform exhibits discrete layer lines at

$$q_z = \frac{2\pi}{p}\, m, \quad m \in \mathbb{Z},$$

with the transverse profile of each line modulated by Bessel functions $J_m(Rq_\perp)$.

2 Theoretical Derivation

2.1 Modeling the Double Helix

We model the double helix by representing each strand as an infinitely thin wire whose electron density is confined to a helical curve. The parametric equations for the two strands are

$$\begin{aligned}\mathbf{r}_1(t) &= \Big(R\cos t,\ R\sin t,\ \frac{p}{2\pi}\, t\Big),\\ \mathbf{r}_2(t) &= \Big(R\cos(t+\pi),\ R\sin(t+\pi),\ \frac{p}{2\pi}\, t\Big),\end{aligned}$$

where R is the helix radius, p is the pitch (the distance along z per full turn), and $t \in \mathbb{R}$. The two strands are separated by a phase shift of π (half a turn). The overall scattering density is then given by

$$\rho(\mathbf{r}) = \int_{-\infty}^{\infty} \delta\Big(\mathbf{r} - \mathbf{r}_1(t)\Big)\, dt + \int_{-\infty}^{\infty} \delta\Big(\mathbf{r} - \mathbf{r}_2(t)\Big)\, dt.$$

2.2 Fourier Transform and Diffraction Amplitude

Under the Fraunhofer approximation, the diffraction amplitude $F(\mathbf{q})$ at scattering vector $\mathbf{q}$ is given by the three-dimensional Fourier transform of $\rho(\mathbf{r})$:

$$F(\mathbf{q}) = \int d^3r\, \rho(\mathbf{r})\, e^{-i\,\mathbf{q}\cdot\mathbf{r}}.$$

Substituting the expression for $\rho(\mathbf{r})$ gives

$$F(\mathbf{q}) = \int_{-\infty}^{\infty} e^{-i\,\mathbf{q}\cdot\mathbf{r}_1(t)}\, dt + \int_{-\infty}^{\infty} e^{-i\,\mathbf{q}\cdot\mathbf{r}_2(t)}\, dt.$$

Assuming the incident beam travels along $+z$ (normal incidence) and the helix is aligned along z, we write the scattering vector as

$$\mathbf{q} = (q_x, q_y, q_z),$$

and define the transverse component

$$q_\perp = \sqrt{q_x^2 + q_y^2}, \quad \phi = \tan^{-1}\left(\frac{q_y}{q_x}\right).$$

For the first strand, we have

$$\mathbf{q}\cdot\mathbf{r}_1(t) = q_x\, R\cos t + q_y\, R\sin t + q_z\, \frac{p}{2\pi}\, t.$$

For the second strand, using $\cos(t+\pi) = -\cos t$ and $\sin(t+\pi) = -\sin t$, we obtain

$$\mathbf{q}\cdot\mathbf{r}_2(t) = -\big(q_x\, R\cos t + q_y\, R\sin t\big) + q_z\, \frac{p}{2\pi}\, t.$$

Expressing the transverse term in polar form,

$$q_x\,\cos t + q_y\,\sin t = q_\perp\,\cos(t-\phi),$$

we rewrite the exponentials as

$$\begin{aligned} e^{-i\,\mathbf{q}\cdot\mathbf{r}_1(t)} &= e^{-i\left[Rq_\perp\,\cos(t-\phi) + \frac{p}{2\pi} q_z\, t\right]}, \\ e^{-i\,\mathbf{q}\cdot\mathbf{r}_2(t)} &= e^{-i\left[-Rq_\perp\,\cos(t-\phi) + \frac{p}{2\pi} q_z\, t\right]}. \end{aligned}$$

2.3 Expansion Using the Jacobi–Anger Identity

To handle the cosine term, we apply the Jacobi–Anger expansion:

$$e^{-iRq_\perp\,\cos(t-\phi)} = \sum_{n=-\infty}^{\infty} (-i)^n\, J_n(Rq_\perp)\, e^{-in(t-\phi)}.$$

Similarly,

$$e^{iRq_\perp\,\cos(t-\phi)} = \sum_{n=-\infty}^{\infty} i^n\, J_n(Rq_\perp)\, e^{-in(t-\phi)}.$$

Substituting these expansions into the integrals, we obtain

$$F_1(\mathbf{q}) = \sum_{n=-\infty}^{\infty} (-i)^n\, J_n(Rq_\perp)\, e^{in\phi} \int_{-\infty}^{\infty} e^{-i\left(n+\frac{p}{2\pi}q_z\right)t}\, dt,$$

$$F_2(\mathbf{q}) = \sum_{n=-\infty}^{\infty} i^n\, J_n(Rq_\perp)\, e^{in\phi} \int_{-\infty}^{\infty} e^{-i\left(n-\frac{p}{2\pi}q_z\right)t}\, dt.$$

Using the Fourier integral identity

$$\int_{-\infty}^{\infty} e^{-i\omega t}\, dt = 2\pi\, \delta(\omega),$$

the t-integrals yield

$$F_1(\mathbf{q}) = 2\pi \sum_{n=-\infty}^{\infty} (-i)^n\, J_n(Rq_\perp)\, e^{in\phi}\, \delta\Big(n + \frac{p}{2\pi}q_z\Big),$$

$$F_2(\mathbf{q}) = 2\pi \sum_{n=-\infty}^{\infty} i^n\, J_n(Rq_\perp)\, e^{in\phi}\, \delta\Big(n - \frac{p}{2\pi}q_z\Big).$$

2.4 Emergence of Layer Lines

The delta functions impose the conditions

$$n = -\frac{p}{2\pi} q_z \quad \text{or} \quad n = \frac{p}{2\pi} q_z.$$

Letting $m = n$, nonzero contributions occur only when

$$q_z = \frac{2\pi}{p} m, \quad m \in \mathbb{Z}.$$

Thus, the diffraction amplitude is nonzero only on these discrete "layer lines" in reciprocal space. The transverse amplitude along each layer line is modulated by the Bessel function $J_m(Rq_\perp)$. Therefore, the intensity,

$$I(\mathbf{q}) = \left|F(\mathbf{q})\right|^2,$$

exhibits horizontal bands in the (q_x, q_z) plane at $q_z = \frac{2\pi}{p} m$, with each band's transverse profile given by $[J_m(Rq_\perp)]^2$.

3 Simulation and Discussion

Figure 2 shows a simulated diffraction intensity map $I(q_x, q_z)$ for the double helix under normal incidence, reproducing the characteristic pattern of Photo 51. In the simulation, each ideal delta function $\delta\Big(q_z - \frac{2\pi}{p} m\Big)$ is approximated by a narrow Gaussian with width σ so that the discrete layer lines appear as horizontal stripes. The brightest band (typically corresponding to $m = 0$) is located at $q_z = 0$, with additional bands appearing at integer multiples of $2\pi/p$.

This derivation relies on the Fraunhofer approximation, which is justified when the detector is sufficiently far from the sample such that the phase variations over the aperture can be approximated linearly. Under these conditions, the diffracted field is given by the Fourier transform of the sample's electron density, and the intensity is the squared magnitude of this transform. This result is fundamental to the field of crystallography and diffraction-based imaging methods [5].

By choosing the coordinate system such that the helix axis and the incident beam are aligned along the z-axis, the mathematical treatment is simplified without loss of generality. Any experimental configuration with oblique incidence can be rotated into this frame, preserving the intrinsic features of the diffraction pattern.

4 Conclusion

We have derived the diffraction pattern of a double helix under Fraunhofer conditions, showing that the far-field intensity is given by the squared magnitude of the Fourier transform of the helical density. The derivation, based on standard approximations and the Jacobi–Anger expansion, demonstrates that the diffraction amplitude is nonzero only along discrete

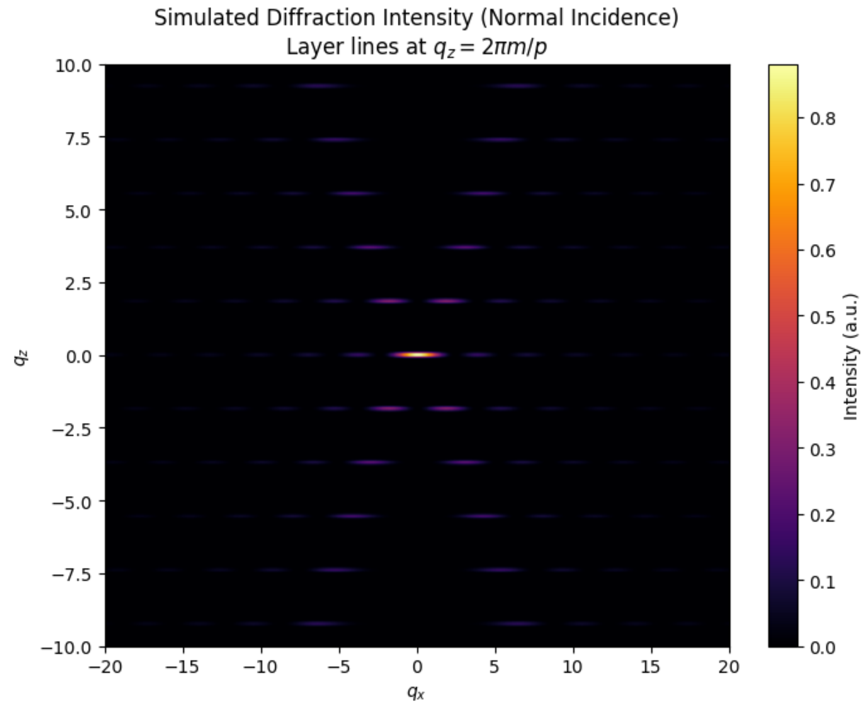

Figure 2: Simulated diffraction intensity for a double helix under normal incidence. Layer lines appear at $q_z = \frac{2\pi}{p} m$.

layer lines at $q_z = \frac{2\pi}{p} m$, with the transverse profile modulated by Bessel functions. This analysis not only explains the classical features observed in Photo 51 but also reinforces the fundamental principle that, under the Fraunhofer approximation, the diffraction intensity is directly related to the Fourier transform of the scattering object.

5 Acknowledgements

Sections of this document, including some calculations and code, were generated and revised with ChatGPT (OpenAI, 2025).

Appendix: Simulation Code

Below is the Python code used to generate Figure 2. It sets up a two-dimensional (q_x, q_z) grid, sums over layer-line indices m, and approximates each ideal delta function by a narrow Gaussian.

```
import numpy as np
import matplotlib.pyplot as plt
from scipy.special import jv

# Parameters
```

```
R = 1.0      # Helix radius
p = 3.4      # Helix pitch
M = 5        # Indices from -M to M
sigma = 0.05 # Gaussian width to mimic delta function

# q-space grid
qx_min, qx_max = -20, 20
qz_min, qz_max = -10, 10
Nqx, Nqz = 400, 400

qx = np.linspace(qx_min, qx_max, Nqx)
qz = np.linspace(qz_min, qz_max, Nqz)
QX, QZ = np.meshgrid(qx, qz)

# Compute intensity
I_normal = np.zeros_like(QX)
for m in range(-M, M+1):
    envelope = jv(m, R * np.abs(QX))**2
    layer = np.exp(-((QZ - (2*np.pi*m/p))**2)/(2*sigma**2))
    I_normal += envelope * layer

# Plot
plt.figure(figsize=(8,6))
plt.imshow(I_normal, origin='lower', extent=[qx_min, qx_max, qz_min, qz_max],
           aspect='auto', cmap='inferno')
plt.xlabel(r'$q_x$')
plt.ylabel(r'$q_z$')
plt.title('Simulated Diffraction Intensity (Normal Incidence)\nLayer lines at $q_z=2\\pi
plt.colorbar(label='Intensity (a.u.)')
plt.show()
```

References

[1] Watson, J. D., & Crick, F. H. C. (1953). Molecular Structure of Nucleic Acids: A Structure for Deoxyribose Nucleic Acid. *Nature, 171*(4356), 737–738.

[2] Wilkins, M. H. F. (1974). *The Third Man of the Double Helix*. Oxford University Press.

[3] Born, M., & Wolf, E. (1999). *Principles of Optics* (7th ed.). Cambridge University Press.

[4] Goodman, J. W. (2005). *Introduction to Fourier Optics* (3rd ed.). Roberts & Company Publishers.

[5] Osgood, B. G. (2019). *The Lectures on Fourier Transform and Its Applications*. IAS/Park City Mathematics Series/AMS.